NRC·CNRC

NRC Publications Archive
Archives des publications du CNRC

Oxidative release of thiol-conjugated forms of the mycotoxin 4-deoxynivalenol

Uhlig, Silvio; Ivanova, Lada; Miles, Christopher O.

This publication could be one of several versions: author's original, accepted manuscript or the publisher's version. / La version de cette publication peut être l'une des suivantes : la version prépublication de l'auteur, la version acceptée du manuscrit ou la version de l'éditeur.
For the publisher's version, please access the DOI link below./ Pour consulter la version de l'éditeur, utilisez le lien DOI ci-dessous.

Publisher's version / Version de l'éditeur:
https://doi.org/10.1021/acs.chemrestox.9b00385
Chemical Research in Toxicology, 33, 2, pp. 515-521, 2019-12-23

NRC Publications Archive Record / Notice des Archives des publications du CNRC :
https://nrc-publications.canada.ca/eng/view/object/?id=b7ff5f3a-27cd-462c-b04d-56aec3a104db
https://publications-cnrc.canada.ca/fra/voir/objet/?id=b7ff5f3a-27cd-462c-b04d-56aec3a104db

Access and use of this website and the material on it are subject to the Terms and Conditions set forth at
https://nrc-publications.canada.ca/eng/copyright
READ THESE TERMS AND CONDITIONS CAREFULLY BEFORE USING THIS WEBSITE.

L'accès à ce site Web et l'utilisation de son contenu sont assujettis aux conditions présentées dans le site
https://publications-cnrc.canada.ca/fra/droits
LISEZ CES CONDITIONS ATTENTIVEMENT AVANT D'UTILISER CE SITE WEB.

Questions? Contact the NRC Publications Archive team at PublicationsArchive-ArchivesPublications@nrc-cnrc.gc.ca. If you wish to email the authors directly, please see the first page of the publication for their contact information.

Vous avez des questions? Nous pouvons vous aider. Pour communiquer directement avec un auteur, consultez la première page de la revue dans laquelle son article a été publié afin de trouver ses coordonnées. Si vous n'arrivez pas à les repérer, communiquez avec nous à PublicationsArchive-ArchivesPublications@nrc-cnrc.gc.ca.

National Research Council Canada | Conseil national de recherches Canada

Canada

Chemical Research in Toxicology

Article

Cite This: Chem. Res. Toxicol. 2020, 33, 515−521

pubs.acs.org/crt

Oxidative Release of Thiol-Conjugated Forms of the Mycotoxin 4-Deoxynivalenol

Silvio Uhlig,*[,†] Lada Ivanova,[†] and Christopher O. Miles[‡]

[†]Toxinology Research Group, Norwegian Veterinary Institute, Ullevålsveien 68, 0454 Oslo, Norway

[‡]Biotoxin Metrology, National Research Council, 1411 Oxford Street, Halifax, NS B3H 3Z1, Canada

Supporting Information

ABSTRACT: Deoxynivalenol (DON) is a trichothecene mycotoxin that is produced by several species of *Fusarium*, which may infect grain crops. DON, as well as other type-B trichothecenes, contain an α,β-unsaturated carbonyl group that may react with sulfhydryl groups in, for example, amino acids and peptides. Such conjugates have been shown to occur in plants. Nucleophilic addition of thiols to the conjugated double bond in DON afforded several isomeric reaction products, and the thermodynamically favored isomers of DON-10-cysteine and DON-10-glutathione have been prepared and characterized previously. This study reports the preparation and characterization of the kinetically favored DON-10-cysteine isomer. We subsequently studied and compared the rate of the deconjugation reaction of the two DON-10-cysteine isomers and the thermodynamically favored DON-10-glutathione adduct. The deconjugation rate of the thermodynamically favored thiol conjugates was slow with half-lives of weeks even at pH 10.7, while the kinetically favored DON-10-cysteine isomer deconjugated within a few hours, affording free DON. We adapted a simple and rapid oxidation protocol in which the sulfide linkage was oxidized to a sulfoxide or sulfone that, when treated with the base, rapidly eliminated the adducted thiol as its sulfenate or sulfinate to afford free DON. The deconjugation reactions of the sulfoxides and sulfones of thermodynamically favored DON-10-thiols were complete within hours or minutes at pH 10.7, respectively. The increase in deconjugation rates for the kinetically favored DON-10-cysteine were less dramatic. Oxidation of sulfides to sulfoxides is known to occur in vivo, and thus, our data show that thiol-conjugated DON might become bioavailable via sulfide oxidation followed by elimination to regenerate DON. The oxidation−elimination approach could also be useful for the indirect quantification of DON-10-thiol conjugates in plant and animal tissues.

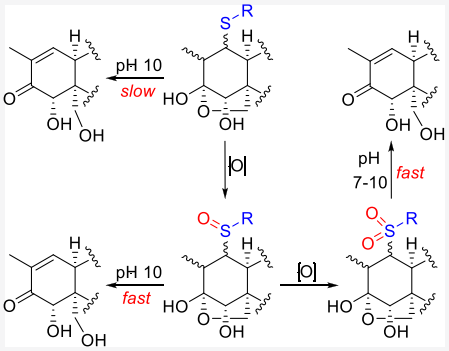

INTRODUCTION

Deoxynivalenol (DON, Figure 1) is a trichothecene mycotoxin and a common contaminant of cereal grain and grain-based products worldwide.[1] Its adverse effects on protein synthesis and the immune system, among other things, has been the subject of numerous studies.[2,3] We have recently shown that DON may undergo reversible Michael addition to the 9,10-olefinic group and irreversible addition to the C-13 epoxide group using thiols as nucleophiles.[4] Such thiol-adducts of DON, e.g. adducts with glutathione and breakdown products thereof, have been shown to occur naturally in plants and cell cultures.[5−7] In our previous studies, we focused on the thermodynamically most stable DON-10-thiol adducts, which are relatively slowly forming reaction products that may be obtained at room temperature and at slightly basic pH.[4,8,9] However, the Michael-addition of thiols to C-10 in DON is dynamic, and several transient adducts can be observed at elevated pH within hours.[4] The glutathione-mediated detoxification of DON is likely secondary in plants and could also be due to chemical reaction rather than being catalyzed by enzymes.[8] However, DON can react with free thiols and thus might conjugate to, for example, peptides and proteins that exhibit free sulfhydryl groups. Such conjugates of DON could be present in tissue samples and might be a useful biomarker of previous exposure. The Michael addition of thiols to the α,β-unsaturated carbonyl moiety in DON is a reversible reaction.[4,10,11] Thus, DON may be released from DON-10-thiols by treatment with a base. This has been shown to occur with other toxins that may undergo Michael addition to thiols, such as the microcystins.[12] The kinetics for the deconjugation reaction of such Michael adducts were relatively slow but were significantly higher after oxidation of the sulfide linkage to a sulfoxide or sulfone.[12]

The objectives of this study were to determine the structure of the fast-forming, and thus kinetically favored, DON-10-cysteine isomer and to establish the deconjugation kinetics of both the kinetically and thermodynamically favored DON-10-cysteine adducts, in addition to that of the thermodynamically favored DON-10-glutathione adduct. Another objective was to compare the rates of the deconjugation reactions for the adducts with those of their corresponding sulfoxides and sulfones.

Received: September 19, 2019
Published: December 23, 2019

Downloaded via NATL RESEARCH COUNCIL CANADA on July 17, 2020 at 13:21:07 (UTC).
See https://pubs.acs.org/sharingguidelines for options on how to legitimately share published articles.

© 2019 American Chemical Society

DOI: 10.1021/acs.chemrestox.9b00385
Chem. Res. Toxicol. 2020, 33, 515−521

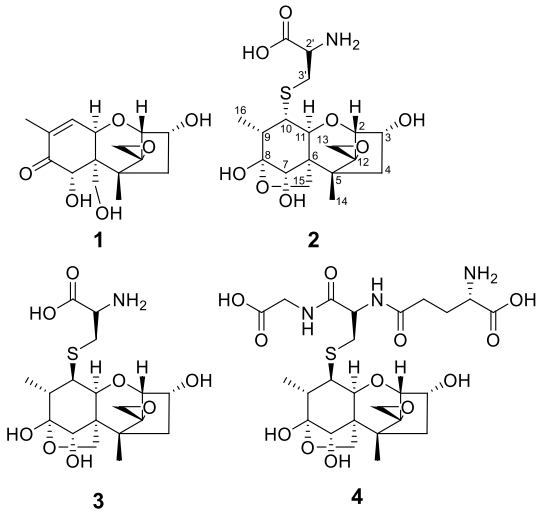

Figure 1. Chemical structures of 4-deoxynivalenol (DON, **1**), the kinetically and thermodynamically favored conjugates of DON-10-cysteine (**2** and **3**, respectively), and the thermodynamically favored DON-10-glutathione conjugate (**4**). The predominant isomer in aqueous solution (ketone vs hemiketal) is shown.

MATERIALS AND METHODS

Chemicals and Reagents. DON (**1**, ≥98%), L-cysteine (≥98%), 5.0 mm Norell Standard Series NMR tubes, D_2O (99.9 atom % D), and sodium carbonate (pro analysis) were from Sigma-Aldrich (Steinheim, Germany). LC−MS grade water and methanol were from Fisher Scientific (Oslo, Norway), whereas ammonium formate (puriss p.a. for HPLC) was from Fluka (Steinheim, Germany). Sodium bicarbonate and sodium carbonate (both pro analysis, Merck, Darmstadt, Germany) were used to prepare 0.2 M carbonate buffers (pH 9.4 and 10.7). Phosphate-buffered saline (PBS, pH 7.3, 0.17 M) was prepared from ready-to-use tablets (Oxoid, Hampshire, U.K.). Acetic acid-d_4 (99.5 atom-% D) was from Cambridge Isotope Laboratories (Tewksbury, MA, United States). Methanol for solid-phase extraction (SPE) was from Romil (Cambridge, U.K.).

Synthesis of the Kinetically Favored DON-10-Cysteine Adduct. 1 (1 mg) was dissolved in 1 mL of a freshly prepared 300 mM solution of L-cysteine in 1% formic acid in a screw-cap vial. The mixture was placed in a heating block adjusted to 40 °C. After 5 days, the vial was removed from the heating block and placed at −26 °C until solid-phase extraction. A 500 mg Strata-X column (Phenomenex, Torrance, CA) was conditioned with 10 mL of methanol followed by 10 mL of water, and the reaction mixture was applied to the column. The vial was washed with 1 mL of water and applied to the Strata-X column. The column was eluted with 10 mL of water followed by 10 mL portions of 2% and 7% methanol in water and then 5 mL of 15% methanol in water. To all fractions, 2 μL of acetic acid was added to stabilize the DON-10-cysteine adduct. The highest proportion of **2** was eluted with 15% methanol, which was partly evaporated under a gentle stream of nitrogen (60 °C), and finally dried by freeze-drying.

NMR Spectroscopy. One-dimensional (1H, JMOD, and DEPT135) and two-dimensional (COSY, TOCSY, HSQC, HMBC, and ROESY) NMR experiments were conducted at 304.6 K using an Avance AVII 600 MHz NMR spectrometer (Bruker BioSpin GmbH, Rheinstetten, Germany) equipped with a 5 mm CP-TCI ($^1H/^{13}C$, $^{15}N-^2H$) triple-resonance inverse cryoprobe with Z-gradient coils. **2** was dissolved in ca. 550 μL of D_2O to which 5 μL of acetic acid-d4 had been added. Data were recorded and processed using Bruker TopSpin (version 3.0), and chemical shifts are reported relative to internal CD_2HCOOD, 2.08 ppm, and CD_3COOD, 21.03 ppm (Table 1).

Molecular Modeling. 3D models of the hemiketal isomer of **2** were constructed and optimized using Chem3D Pro version 16 (PerkinElmer Informatics, Inc., Waltham, MA) and PyMOL version 2.2.3 (Schrödinger, New York, NY).

Table 1. ^1H and ^{13}C NMR Assignments (δ in ppm, Relative to Internal CHD_2CO_2D at 2.08 ppm and CD_3CO_2D at 21.03 ppm) for the Kinetically Favored DON−Cysteine Michael Adduct (2) in D_2O with CD_3CO_2D (1% v/v)[a]

	2 (hemiketal)		**2** (ketone)	
atom	^1H	^{13}C	^1H	^{13}C
2	3.68 (d, 4.6)	82.6	3.75 (d, 4.6)	81.9[b]
3	4.49 (dt, 11.2, 4.5)	69.4	4.46 (m)	69.4[b]
4	1.95 (dd, 14.8, 4.5)2.07 (dd, 14.8, 11.2)	45.2	2.06[c] (dd, 14.8, 5.5) 2.73 (dd, 14.8, 4.4)	n.o.[d]
5	–	44.3	–	47.4[b]
6	–	56.7	–	56.6[b]
7	4.04 (s)	77.7	4.95 (s)[f]	76.1[b,f]
8	–	107.7	–	215.3[e]
9	2.55 (dq, 7.8, 7.3)	40.8	3.55 (m)	42.6[d]
10	3.12 (br d, 7.3)	51.9	3.63 (dd, 6.8, 2.2)	55.9[d]
11	4.88 (br s)	81.9	4.91 (br s)[f]	77.8[b,f]
12	–	68.5	–	68.4[e]
13	3.25 (d, 3.7)3.30 (d, 3.7)	49.2	3.20 (m)3.23 (m)	49.3[b]
14	1.05 (s)	15.3	1.07 (s)	14.4[b]
15	4.22 (s)	68.3	3.56 (d, 13.5)4.02 (d, 13.5)[g]	61.4[b]
16	1.10 (d, 7.2)	13.8	1.19 (d, 6.8)	12.1[b]
1′	–	173.5	–	n.o.[d]
2′	4.01 (dd, 9.2, 3.6)	54.9	3.98 (dd, 7.6, 4.4)	54.9[b]
3′	3.09 (dd, 15.1, 9.2)3.19 (dd, 15.1, 5.1)	34.5	3.15 (dd, 13.5, 6.8)3.32 (dd, 13.5, 3.9)	n.o.[d]

[a]In the format: chemical shift in ppm (multiplicity, coupling constants in Hz). [b]Chemical shift measured from HSQC spectrum. [c]Chemical shift measured from COSY spectrum. [d]Not observed. [e]Chemical shift measured from HMBC spectrum. [f]Might be interchanged. [g]Coupling constant measured from HSQC spectrum.

LC−HRMS. Separation was achieved using a 150 × 2.1 mm i.d., 2.6 μm Kinetex F5 column (Phenomenex). The mobile phase (250 μL/min) consisted of 5 mM ammonium formate (A) and 5 mM ammonium formate in 95:5 methanol−water (B). The column was eluted using a linear gradient from 3%−40% B over 14.5 min, then to 100% B at 14.7 min (2 min hold), followed by return to 3% B at 16.9 min and equilibration with 3% B for 3.1 min using a Vanquish Horizon UHPLC pump (Thermo Fischer Scientific, Waltham, MA). The mass analyzer was a Q-Exactive Fourier-transform high-resolution mass spectrometer (Thermo Fischer Scientific) equipped with a heated electrospray ionization interface (HESI-II). The mass spectrometer was run in positive and negative ion full-scan mode using fast polarity switching (i.e., alternating positive and negative ion scans), in the mass range m/z 150−1200. The mass resolution was set to 70 000 at m/z 200. The spray voltage was 4 kV, and the transfer capillary temperature was 250 °C; the sheath and auxiliary gas flow rates were 35 and 10 units, respectively. Parallel reaction monitoring was performed using a 2 m/z quadrupole isolation window, a mass resolution of 17 500 at m/z 200, and a normalized collision energy of 30%. Exact values of m/z used for extracted ion LC−HRMS chromatograms for DON-thiol conjugates and their sulfoxides and sulfones (Table 2) were obtained using *Fusarium* toxin mass calculator version 9,[13] while Xcalibur 2.3 or 3.0 (Thermo Fisher Scientific) was used to calculate mass errors.

Oxidation of DON-10-Thiols to Their Sulfoxides and Sulfones using Oxone. An aliquot (50 or 100 μL) of an 8.6 μg/mL stock solution of **4** or 0.51 μg/mL **3** in water was transferred to a chromatography vial and diluted with 450 or 900 μL of water, respectively. A fresh solution of Oxone (10 mg/mL) was prepared in water, and 50 μL was added to the chromatography vial and vortexed. The vial was placed in the UHPLC autosampler, which was thermostated to 20 °C, and aliquots were injected every 23 min in order to monitor the progress of thiol oxidation (Figure 2). The procedures were identical for **2**; however, the exact concentration was

DOI: 10.1021/acs.chemrestox.9b00385
Chem. Res. Toxicol. 2020, 33, 515−521

Table 2. Accurate Masses of Oxidized DON-Thiols Obtained from LC−HRMS Analysis

compound	$t_{R\ (min)}$	ion	m/z found	formula	Δm (ppm)
2-sulfoxide (**2(O)**)	3.75	$[M + H]^+$	434.1473	$C_{18}H_{28}NO_9S$	−1.5
2-sulfone (**2(O_2)**)	4.34	$[M + H]^+$	450.1422	$C_{18}H_{28}NO_{10}S$	−1.4
3-sulfoxide a (**3(O)a**)	3.40	$[M + H]^+$	434.1483	$C_{18}H_{28}NO_9S$	0.88
3-sulfoxide b (**3(O)b**)	4.47	$[M + H]^+$	434.1484	$C_{18}H_{28}NO_9S$	1.2
3-sulfone (**3(O_2)**)	4.98	$[M + H]^+$	450.1431	$C_{18}H_{28}NO_{10}S$	0.50
4-sulfoxide a (**4(O)a**)	2.26	$[M + H]^+$	620.2120	$C_{25}H_{38}N_3O_{13}S$	1.7
4-sulfoxide b (**4(O)b**)	2.82	$[M + H]^+$	620.2131	$C_{25}H_{38}N_3O_{13}S$	1.9
4-sulfone (**4(O_2)**)	3.28	$[M + H]^+$	636.2079	$C_{25}H_{38}N_3O_{14}S$	1.5

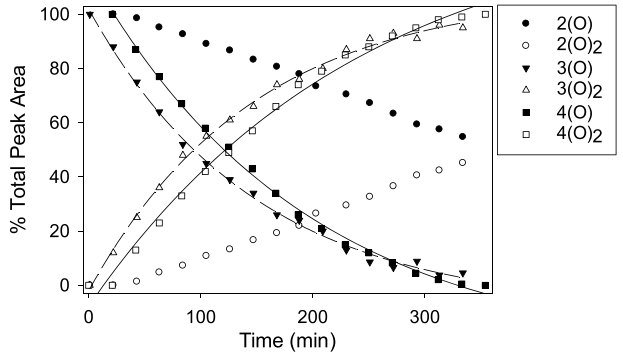

Figure 2. Oxidation reaction of the two DON-10-cysteine diastereoisomers (**2** and **3**) and DON-10-glutathione (**4**) with Oxone at 20 °C via their sulfoxides (**2(O)**−**4(O)**) to their sulfones (**2(O_2)**−**4(O_2)**) over a time period of 6 h. The DON-thiols were oxidized to sulfoxides immediately upon addition of Oxone.

not known, and concentrations were adjusted so the peak height of $[M + H]^+$ was in the same range as that of **3**.

Deconjugation of DON-10-Thiols. Aliquots of **2**−**4** (100 μL; 0.51 μg/mL for **3**, 8.6 μg/mL for **4**, and a concentration for **2** so the peak height of $[M + H]^+$ was in the same range as that of **3**), dissolved in water, were transferred to screw-cap chromatography vials with conical inserts. The vials and buffer stock solutions were placed in the thermostated LC−HRMS autosampler for ca. 30 min to allow their temperatures to equilibrate to 20 °C. To the DON-thiol conjugate solutions was added 100 μL of the appropriate buffer solution (i.e., either pH 7.3 PBS or pH 9.4 or pH 10.7 carbonate buffer); the solution was vortex-mixed, and a 1−3 μL aliquot was immediately injected into the LC−HRMS and thereafter injected at appropriate intervals.

Deconjugation of DON-10-Thiols via Oxidation to Sulfoxides. To a 500 μL aliquot of **2**−**4** was added 10 μL of a fresh aqueous solution of Oxone (10 mg/mL), and the mixture was vortex-mixed. An aliquot of DMSO (10 μL) was immediately added, and the mixture was vortexed again. This procedure resulted in practically quantitative oxidation of DON-thiols to their sulfoxides. To the solutions was added 100 μL of the appropriate buffer solution (i.e., pH 7.3 PBS or pH 9.4 or pH 10.7 carbonate buffer); the solution was vortex-mixed, and a 1−3 μL aliquot was immediately injected into the LC−HRMS. Subsequent injections were performed every 23 min.

Deconjugation of DON-10-Thiols via Oxidation to Sulfones. To a 500 μL aliquot of **2**−**4** was added 10 μL of a fresh aqueous solution of Oxone (10 mg/mL); the mixture was vortex-mixed and placed in the autosampler thermostated to 20 °C. The progress of the oxidation reaction was monitored by LC−HRMS. After 5−6 h, 10 μL of DMSO as well as 500 μL of pH 7.3 PBS or pH 9.4 or pH 10.7 carbonate buffer (pre-equilibrated to 20 °C) was added, and the mixture was vortex-mixed.

Kinetic Analyses. Half-lives of sulfide-, sulfoxide-, and sulfone-conjugates in each deconjugation reaction were calculated by fitting their absolute abundances (peak areas) to 2-parameter exponential decay curves (SigmaPlot 14.0, Systat Software Inc., San Jose, CA).

RESULTS AND DISCUSSION

We have previously shown that the nucleophilic addition of thiols to C-10 in DON is dynamic, with several isomers formed at different rates.[4] Because this reaction is reversible, we anticipated that the observed dynamic nature of the reaction is the result of different rates for the forward (i.e., conjugation) and reverse (i.e., elimination of the thiol) reactions of the isomers involved. In order to study the reverse reaction for isomeric DON-10-thiol conjugates, we aimed to synthesize and purify the kinetically favored DON-10-cysteine isomer (**3**), while its thermodynamically more stable isomer as well as the thermodynamically stable DON-10-glutathione isomer (**4**) were available from previous work.[8,9] The synthesis was achieved by reaction of DON with L-cysteine in 1% aqueous formic acid at slightly elevated temperature. Acidic reaction conditions were chosen in order to slow down the nucleophilic

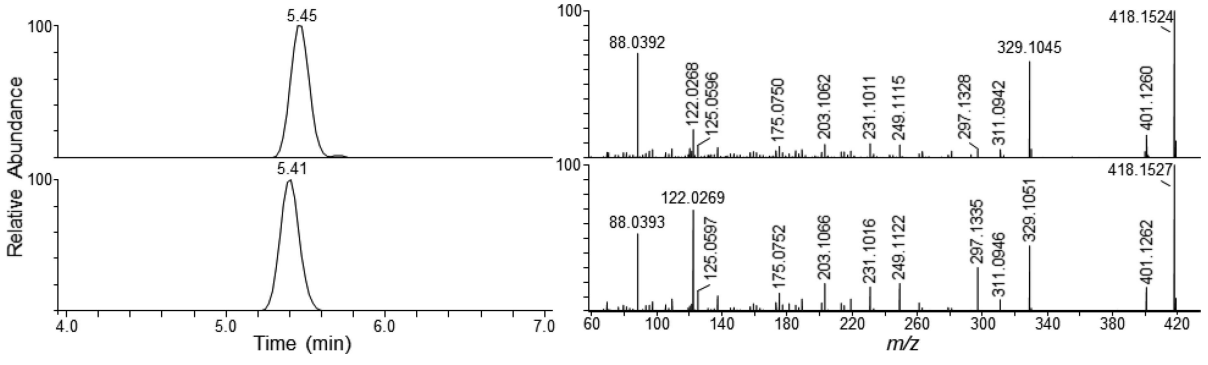

Figure 3. Extracted ion chromatograms (±3 ppm) from LC−HRMS of the $[M + H]^+$ ions (m/z 418.1530) of DON-10-cysteine obtained from reaction in aqueous formic acid (upper trace) and from reaction in pH 10.7 carbonate buffer for 2 h (lower trace). HRMS/MS spectra are from higher-energy collision dissociation of $[M + H]^+$.

DOI: 10.1021/acs.chemrestox.9b00385
Chem. Res. Toxicol. 2020, 33, 515−521

addition of the thiol, thereby allowing for better control of the reaction. The reaction mixture was then easily separated using SPE because after a reaction time of 5 days other diastereoisomers had not started to be formed. Furthermore, comparison of the LC−HRMS(/MS) characteristics of the DON-10-cysteine isomer obtained in formic acid were consistent with those observed for the transient product observed during reaction in carbonate buffer after a reaction time of 2 h (Figure 3).

Structure Elucidation. The chemical structure of DON-10-cysteine adduct **2** (Figure 1) was determined using NMR spectroscopy. As explained in previous communications, the sample was dissolved in D_2O/CD_3COOD because acid was necessary to stabilize the adduct.[4,8,9] The ketone/hemiketal ratio was 14:86 based on measurements of the areas under the two methyl peaks (H-14, 1.07, and 1.05 ppm; and H-16, 1.19, and 1.10 ppm, respectively) (Table 1). The proportion of the hemiketal isomer was thus higher for the kinetically favored DON-10-cysteine adduct compared to the thermodynamically most stable adduct (14:86 vs 29:71 ketone/hemiketal for the kinetically favored vs the thermodynamically favored isomer).[9] The ^1H and ^{13}C chemical shifts of hemiketal **2** were similar to those of the hemiketal isomer of the thermodynamically stable DON-10-cysteine isomer **3**, apart from resonances arising from positions 9−11 (Table 1).[9] The largest change in observed ^{13}C chemical shifts in **2** relative to **3** was observed for C-11. The chemical shift for C-11 was changed by +6.4 ppm in **2** relative to **3**, while the ^1H chemical shift for H-11 was changed by −0.29 ppm (Table 1).[9] The largest change in ^1H chemical shifts was observed for H-9, for which the ^1H chemical shift was changed by +0.69 ppm in **2** relative to **3**, while the corresponding ^{13}C chemical shift was changed by +2.2 ppm (Table 1).[9] Another notable feature of the NMR spectra was a decrease in the $^3J_{H-H}$ coupling constant between H-9 and H-10 in **2** (7.3 Hz) relative to the corresponding coupling constant in **3** (11.9 ppm). The relatively large $^3J_{H-H}$ coupling constant between H-9 and H-10 in the case of the slowly forming, thermodynamically favored adduct can be explained by a dihedral angle between H-9 and H-10 of close to 180°,[14] while the $^3J_{H-H}$ coupling constant in **2** indicates a dihedral angle between the two vicinal protons close to 0°. The stereochemistry at C-9 and C-10 was further studied using ROESY NMR spectra (Figure S3). The ROESY NMR spectra showed NOE correlations between H-9 (2.55 ppm) and H-7 (4.04 ppm), H-10 (3.12 ppm), and H-16 (1.10 ppm), while H-10 showed NOE correlations to H-9 (2.55 ppm), H-11 (4.88 ppm), and H-16 (1.10 ppm) (Figures 4 and S3). In contrast, the ROESY NMR spectrum of **3** showed NOE correlations between H-9 and H-7, but not between H-9 and H-10.[9] Thus, these data are consistent with the stereochemistry shown for **2** in Figures 2 and 4, with both H-9 and H-10 on the β-face of the molecule. Furthermore, there was no $^3J_{H-H}$ coupling between H-10 and H-11, indicating a dihedral angle between the two protons of approximately 90° (Figure 4).

The assignment of the chemical shifts for the ketone isomer of **2** was rather ambiguous because of low signal/noise (Table 1). The H-7 and H-11 protons were partially hidden below the residual water peak and observed only in the ^1H-proton NMR spectrum without solvent suppression, as well as in the HSQC spectrum (Table 1). However, because of the lack of correlations in the HMBC or ROESY spectra, the exact assignment of CH-7 and CH-11 was not possible, and the reported ^1H and ^{13}C chemical shift values might be interchanged (Table 1).

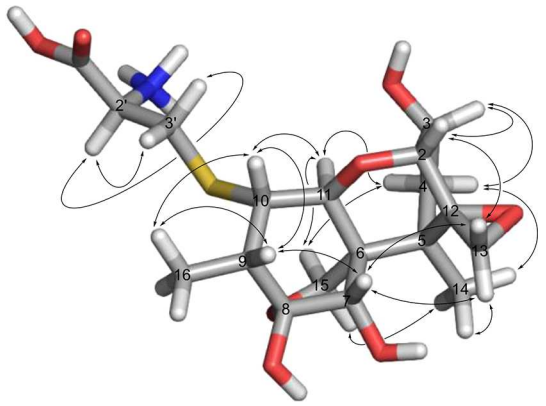

Figure 4. 3D model of the hemiketal form of the DON-10-cysteine Michael adduct **2**, including correlations observed in the ROESY NMR spectrum that corroborate the stereochemistry of **2**.

Deconjugation of DON-10-Thiol Adducts. DON-10-thiols were expected to deconjugate by treatment with base.[15] Having two different DON-10-cysteine diastereoisomers and a DON-10-glutathione adduct allowed us to study and compare the rates of their deconjugation reactions at different pH values. The half-life for the deconjugation of the fast-forming, kinetically favored DON-10-cysteine adduct **2** was several orders of magnitude lower than that of the slowly forming adduct at basic pH (Table 3). For example, while the half-life of **2** at pH 10.7 was 3.3 h, the half-life of the slowly forming diastereoisomer **3** was more than 12 days. At pH 9.4, no measurable deconjugation of **3** occurred over a period of 12 days (Table 3). The half-life for the deconjugation reaction of **4** was comparable, albeit slightly higher than that of **3** (Table 3). This is in line with **3** and **4** having the same stereochemistry at C-9 and C-10. These data suggest that the dynamic properties of the thia-Michael addition to DON is a result of different reaction rates for the formation of different diastereoisomers, as well as of variable rates for the deconjugation reaction of the different isomers. Furthermore, the ketone−hemiketal isomerization will also play a role in controlling the forward and backward reactions.

Deconjugation of DON-10-Thiol Adducts via Oxidation to Sulfoxides and Sulfones. Conversion of the sulfide group in DON-10-thiols to a sulfoxide or sulfone was expected to increase the rate of the base-catalyzed deconjugation reaction (Figure 5). For example, the rapid release of thiol-conjugated microcystins after oxidation of the sulfide linkage has recently been shown.[12] The rationale for developing such a protocol is the possibility for release and subsequent analysis of thiol-bound toxins, e.g. toxins that are bound to the cysteinyl moieties in proteins and peptides. The sulfoxides **2(O)**−**4(O)** and sulfones **2(O_2)**−**4(O_2)**, produced by oxidation of the sulfides, were analyzed by LC−HRMS (Table 2) to verify that their MS characteristics were consistent with the proposed *S*-oxidation products. All three DON-thiols were readily oxidized to their corresponding sulfoxides and sulfones using Oxone in a one-step reaction.[16] The oxidation to the sulfoxides was virtually instantaneous, while oxidation to the sulfones was complete within ca. 6 h for **3** and **4**, whereas **2** was oxidized to a ca. 1:1 mixture of **2(O)**/**2(O_2)** (Figure 2). The resulting sulfones were stabilized by addition of DMSO in order to consume excess Oxone. Omitting the addition of DMSO led to a substantial loss of the sulfones within 1 day (data not shown), but because of the relatively low amounts of **2**, **3**, and **4** available we did not

DOI: 10.1021/acs.chemrestox.9b00385
Chem. Res. Toxicol. 2020, 33, 515−521

Table 3. Half-Lives (Hours) at 20 °C for the Deconjugation of the Sulfide, Sulfoxide, and Sulfone Forms of DON-10-Thiol Conjugates at Neutral (2 and 3) to Moderately Basic (2−4) pH Calculated from 2-Parameter Exponential Decay Curves

	2			3			4	
pH	7.3	9.4	10.7	7.3	9.4	10.7	9.4	10.7
sulfide	>288[a]	30	3.3		>288[b]	>288[c]	>288[b]	432[d]
sulfoxides	>50[e]	15	1.2	4.9/8.5	0.84/0.70	0.93/0.73	182/101[g]	35/10
sulfone	13	2.0	0.45	0.53	ca. 0.05[f]	ca. 0.05[f]	3.9	0.52

[a]15% reduction of peak area of **2** after 12 days. [b]No reduction of peak area after 12 days. [c]23% reduction of peak area of **3** after 12 days. [d]Estimated from extrapolation of exponential decay curve; 46% reduction in peak area of **3** after 12 days. [e]12% reduction of peak area of **2(O)** after 50 h. [f]**3(O_2)** could not be detected after 22 min (second injection to LC−HRMS); estimation is based on a limit of detection of 1% of starting concentration. [g]Estimated from extrapolation of exponential decay curve; 25%/42% reduction in peak area of **4(O)a/4(O)b** after 94 h (3.9 days)

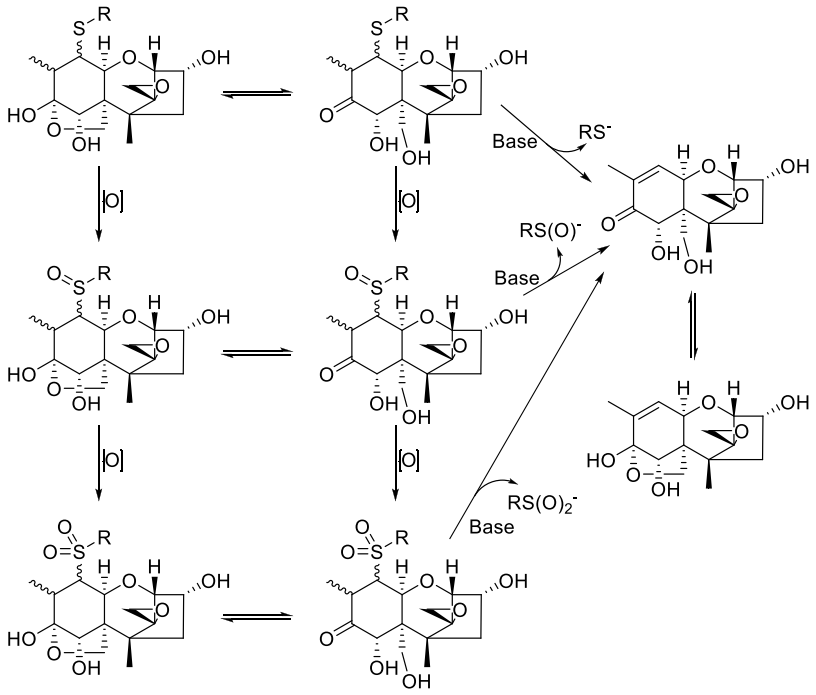

Figure 5. Oxidation of DON-thiols to its sulfoxide and sulfone derivatives and subsequent base-catalyzed elimination of the corresponding sulfenates and sulfinates, respectively. The DON-thiols (**2**−**4**) used in this study behaved in the same manner.

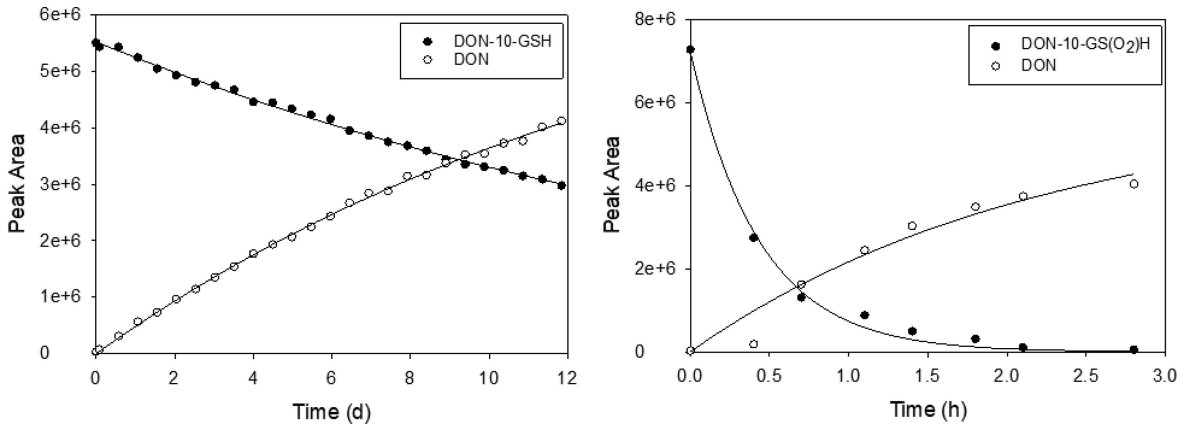

Figure 6. Deconjugation reaction for **4** (left) and **4(O_2)** (right) at pH 10.7 and 20 °C. Concentration data are fitted to 2-parameter exponential decay or rise curves. Note the different scaling of the *x*-axes.

investigate this further. However, DON itself to which 10 μL of a 10 mg/mL solution of Oxone had been added was stable for several days.

Kinetic analysis of the deconjugation of **2**−**4** and their oxidized derivatives showed that the increase in the rate for the deconjugation reaction for the three conjugates after oxidation to their corresponding sulfoxides and sulfones varied substantially (Table 3). The half-life for the deconjugation of the fast-forming DON-10-cysteine adduct **2** was reduced to ca. 20% after oxidation to its sulfoxide (**2(O)**) and to 7−9% after oxidation to

DOI: 10.1021/acs.chemrestox.9b00385
Chem. Res. Toxicol. 2020, 33, 515−521

its sulfone (**2**(O_2)) (Table 3). However, the half-life for the deconjugation of the slowly forming DON-10-cysteine adduct **3** was reduced to less than 0.2% for its sulfoxide (**3**(**O**)) at pH 10.7, and thus the deconjugation half-lives of **2**(**O**) and **3**(**O**) were comparable at that pH (Table 3). Furthermore, the deconjugation of the corresponding sulfone **3**(O_2) at pH 9.4 and 10.7 was complete after the second LC−HRMS analysis, and even at neutral pH it was only about 30 min, indicating a further increase of about an order of magnitude in reactivity relative to sulfoxide **3**(**O**). The stereochemistry along the C-9−C-10 bond in **4** is identical to that in **3**, and similar deconjugation half-lives had been observed for the two DON-thiols. Oxidation of **4** to its sulfoxide **4**(**O**) resulted in a less dramatic increase in the deconjugation rate compared to **3** versus **3**(**O**). Thus, although the deconjugation half-life of **4**(**O**) was reduced to ca. 2−8% of that of **4**, the deconjugation half-life of **4**(**O**) was substantially larger than that of **2**(**O**) (Table 3). Oxidation of **4** to its sulfone **4**(O_2) reduced the deconjugation half-life to less than 0.1%, resulting in comparable deconjugation half-lives for **2**(O_2) and **4**(O_2) at pH10.7, while that of **3**(O_2) was about 1 order of magnitude smaller (Table 3 and Figure 6).

The exact deconjugation kinetics for DON-10-thiols could be rather complicated as several coexisting equilibria will influence the observed rate of the deconjugation reaction (Figure S5). A critical step for the base-catalyzed elimination of the thiol is the attack of the base on the C−H bond in position-9.[17] The acidity of H-9 will depend on whether DON is in its ketone or hemiketal form; that is, the pK_a of H-9 is expected to be lower for the ketone isomer, which will favor base attack (Figure 5).[17] The same equilibrium will also affect the kinetics of the next steps of the deconjugation reaction. Because of the rather complex interrelation of equilibria, increasing the pH has a different effect on the deconjugation rates of **2**−**4** (Table 3). For example, the pH had an effect over the whole pH range studied on the deconjugation kinetics of **2**(**O**), while the half-lives for the deconjugation reaction of **3**(**O**) were not further reduced by increasing the pH from 9.4 to 10.7. The pK_a of H-9 appears therefore to be lower in **3**(**O**) compared to **2**(**O**).

Toxicological Implications and Applications. Thiol conjugation of DON has been shown in plants, and conjugation reactions with thiols such as cysteine-containing peptides and proteins could also be expected in animals and humans. Cereal plants that are infected with certain *Fusarium* spp. may be continuously exposed to DON over weeks.[18] Furthermore, humans or some animals such as pigs that have cereal grains as part of their diet might be exposed to varying concentrations of DON over large periods of their life. This repeated exposure may result in the long-term systemic presence of DON despite the fast elimination kinetics in mammals.[19] The presented approach of releasing DON from possible 10-*S*-conjugates after oxidation using Oxone could be an interesting application for assessing their presence in plant and animal tissues. The thermodynamically favored diastereoisomer of DON-10-*S*-conjugates appears to be relatively stable (i.e., the rate of the reverse reaction is low) at physiological and elevated pH. This is apparently not the case for their oxidized forms. Because sulfide-conjugates undergo slow autoxidation, conjugated DON is likely to be released after *S*-oxidation and then become bioavailable. This could for example occur during oxidative stress. Michael acceptor systems are involved in the metabolism and distribution of other toxins, contaminants, and drugs, e.g., microcystins and acrylamide. The toxicological significance of the thia-Michael addition in the case of the latter two has already been shown, but the potential effects and toxicological consequences of the *S*-oxidation of conjugates of such compounds are poorly understood.[20,21]

■ ASSOCIATED CONTENT

Supporting Information

The Supporting Information is available free of charge at https://pubs.acs.org/doi/10.1021/acs.chemrestox.9b00385.

NMR spectra (^{1}H and ^{13}C NMR, ROESY), scheme showing mechanism of base-catalyzed deconjugation, NOEs in table format (PDF)

LC−HRMS peak areas from extracted ion chromatograms for all deconjugation experiments (XLSX)

■ AUTHOR INFORMATION

Corresponding Author

*Tel.: +47 474 14 232. E-mail: silvio.uhlig@vetinst.no.

ORCID

Silvio Uhlig: 0000-0001-6419-9563

Funding

This work was part of the project DONDetox: Removal of mycotoxins in agriculture, funded by the Research Council of Norway (Grant 249039) and cofinanced by Lantmännen Research Foundation and was partly supported by the Research Council of Norway through the Norwegian NMR Platform, NNP (Grant 226244/F50).

Notes

The authors declare no competing financial interest.

■ ACKNOWLEDGMENTS

We thank Alistair L. Wilkins for assistance in the interpretation of NMR data and molecular modelling.

■ ABBREVIATIONS USED

COSY, correlation spectroscopy; DEPT, distortionless enhancement of polarization transfer; HMBC, heteronuclear multiple bond correlation; HSQC, heteronuclear single-quantum coherence; JMOD, J-modulated spin−echo; NOE, nuclear Overhauser effect; PBS, phosphate-buffered saline; ROESY, rotating frame Overhauser spectroscopy; TOCSY, total correlation spectroscopy

■ REFERENCES

(1) Pascari, X., Marin, S., Ramos, A. J., Molino, F., and Sanchis, V. (2019) Deoxynivalenol in cereal-based baby food production process. A review. *Food Control 99*, 11−20.

(2) Maresca, M. (2013) From the gut to the brain: journey and pathophysiological effects of the food-associated trichothecene mycotoxin deoxynivalenol. *Toxins 5* (4), 784−820.

(3) Pinton, P., and Oswald, I. P. (2014) Effect of deoxynivalenol and other Type B trichothecenes on the intestine: a review. *Toxins 6*, 1615−1643.

(4) Stanic, A., Uhlig, S., Solhaug, A., Rise, F., Wilkins, A. L., and Miles, C. O. (2015) Nucleophilic addition of thiols to deoxynivalenol. *J. Agric. Food Chem. 63*, 7556−7566.

(5) Juan-Garcia, A., Juan, C., Konig, S., and Ruiz, M. J. (2015) Cytotoxic effects and degradation products of three mycotoxins: alternariol, 3-acetyl-deoxynivalenol and 15-acetyl-deoxynivalenol in liver hepatocellular carcinoma cells. *Toxicol. Lett. 235*, 8−16.

(6) Kluger, B., Bueschl, C., Lemmens, M., Michlmayr, H., Malachova, A., Koutnik, A., Maloku, I., Berthiller, F., Adam, G., Krska, R., and Schuhmacher, R. (2015) Biotransformation of the mycotoxin deoxynivalenol in *Fusarium* resistant and susceptible near isogenic wheat lines. *PLoS One 10*, No. e0119656.

DOI: 10.1021/acs.chemrestox.9b00385
Chem. Res. Toxicol. 2020, 33, 515−521

(7) Uhlig, S., Stanic, A., Hofgaard, I. S., Kluger, B., Schuhmacher, R., and Miles, C. O. (2016) Glutathione-conjugates of deoxynivalenol in naturally contaminated grain are primarily linked via the epoxide group. *Toxins 8*, 329−340.
(8) Stanic, A., Uhlig, S., Sandvik, M., Rise, F., Wilkins, A. L., and Miles, C. O. (2016) Characterization of deoxynivalenol-glutathione conjugates using nuclear magnetic resonance spectroscopy and liquid chromatography-high-resolution mass spectrometry. *J. Agric. Food Chem. 64*, 6903−6910.
(9) Stanic, A., Uhlig, S., Solhaug, A., Rise, F., Wilkins, A. L., and Miles, C. O. (2016) Preparation and characterization of cysteine adducts of deoxynivalenol. *J. Agric. Food Chem. 64*, 4777−4785.
(10) Esterbauer, H., Zollner, H., and Scholz, N. (1975) Reaction of glutathione with conjugated carbonyls. *Z. Naturforsch., C: J. Biosci. 30*, 466−473.
(11) Krenske, E. H., Petter, R. C., and Houk, K. N. (2016) Kinetics and thermodynamics of reversible thiol additions to mono- and diactivated michael acceptors: Implications for the design of drugs that bind covalently to cysteines. *J. Org. Chem. 81*, 11726−11733.
(12) Miles, C. O. (2017) Rapid and convenient oxidative release of thiol-conjugated forms of microcystins for chemical analysis. *Chem. Res. Toxicol. 30*, 1599−1608.
(13) Miles, C. O. (2016) *Fusarium toxin mass calculator (version 9 in Excel)*.
(14) Bothner-By, A. A. (1965) Geminal and vicinal proton-proton coupling constants in organic compounds. *Adv. Magn. Opt. Reson. 1*, 195−316.
(15) Miles, C. O., Sandvik, M., Nonga, H. E., Ballot, A., Wilkins, A. L., Rise, F., Jaabaek, J. A., and Loader, J. I. (2016) Conjugation of microcystins with thiols is reversible: base-catalyzed deconjugation for chemical analysis. *Chem. Res. Toxicol. 29*, 860−870.
(16) Parida, K. N., Chandra, A., and Moorthy, J. N. (2016) Oxidation of thiols to sulphonic acids with Oxone/$NaHCO_3$ and $KBrO_3$. *ChemistrySelect 1*, 490−494.
(17) Krishnan, S., Miller, R. M., Tian, B. X., Mullins, R. D., Jacobson, M. P., and Taunton, J. (2014) Design of reversible, cysteine-targeted Michael acceptors guided by kinetic and computational analysis. *J. Am. Chem. Soc. 136*, 12624−12630.
(18) Audenaert, K., Vanheule, A., Hofte, M., and Haesaert, G. (2014) Deoxynivalenol: a major player in the multifaceted response of *Fusarium* to its environment. *Toxins 6*, 1−19.
(19) Faeste, C. K., Ivanova, L., Sayyari, A., Hansen, U., Sivertsen, T., and Uhlig, S. (2018) Prediction of deoxynivalenol toxicokinetics in humans by in vitro-to-in vivo extrapolation and allometric scaling of in vivo animal data. *Arch. Toxicol. 92*, 2195−2216.
(20) Buratti, F. M., Scardala, S., Funari, E., and Testai, E. (2011) Human glutathione transferases catalyzing the conjugation of the hepatoxin microcystin-LR. *Chem. Res. Toxicol. 24*, 926−933.
(21) Tong, G. C., Cornwell, W. K., and Means, G. E. (2004) Reactions of acrylamide with glutathione and serum albumin. *Toxicol. Lett. 147*, 127−131.

DOI: 10.1021/acs.chemrestox.9b00385
Chem. Res. Toxicol. 2020, 33, 515−521